Res Chem Intermed (2011) 37:551–565
DOI 10.1007/s11164-011-0287-x

# Hydrothermal solidification of municipal solid waste incineration fly ash

**Chengchong Shan · Zhenzi Jing · Lili Pan · Lei Zhou · Xiaohui Pan · Lei Lu**

Received: 25 July 2010 / Accepted: 10 November 2010 / Published online: 2 February 2011


**Abstract** Hydrothermal solidification of municipal solid waste incineration (MSWI) fly ash has been conducted under saturated steam pressure at 200 °C for up to 48 h with quartz addition. To enhance the strength of solidified specimens further, the raw fly ash was pre-treated by water-washing and mixed with NaOH solution (2 M) as reaction solvent. Experimental results showed that curing time and temperature had significant effects on strength development. Strength development was found to be mainly due to tobermorite formation, and addition of quartz and NaOH solution promoted tobermorite formation. The raw fly ash could also be used as an additive to solidify MSWI bottom ash, and with raw fly ash addition (10%) the flexural strength of solidified specimens reached more than 21 MPa, suggesting high potential to recycle 100% MSWI ash (e.g. as 10% fly ash + 90% bottom ash). Leaching tests were conducted to determine amounts of heavy metals dissolved from solidified specimens. The results showed that under the hydrothermal conditions of this study, leaching of heavy metals was very low. As such, the hydrothermal processing method might have high potential for recycling/reusing MSWI fly ash on a large scale.

**Keywords** Hydrothermal solidification · MSWI fly ash · Heavy metals leaching · Washing-treatment · Tobermorite

## Introduction

During municipal solid waste incineration (MSWI), solid particles are produced which can be grouped into bottom ash and fly ash. The fly ash, which contains many harmful substances, for example heavy metals and dioxins, is regarded as a

C. Shan · Z. Jing (✉) · L. Pan · L. Zhou · X. Pan · L. Lu
School of Materials Science and Engineering, Tongji University, Shanghai 200092, China
e-mail: zzjing@tongji.edu.cn

hazardous material and treatment to immobilize heavy metals is required before landfill. As the number of incineration facilities in big cities of China, for example Shanghai, Beijing, and Guangzhou, increases, the amount of MSWI fly ash quickly increases. In Shanghai alone, for example, 20,000 ton of MSWI fly ash is produced annually, and the amount is still growing quickly because of industrialization [1]. Because of the shortage of landfill and tighter environmental regulations, the large output of MSWI fly ash has caused various social and environmental problems. Therefore, new ways of treating/utilizing MSWI fly ash are urgently needed.

Although, methods have been developed for treatment of MSWI fly ash, for example vitrification, physical/chemical separation, and stabilization/solidification (S/S) [2–4], few seem applicable on a large scale—thermal treatment of MSWI fly ash by vitrification is regarded as costly, physical/chemical separation methods used to extract heavy metals from fly ash are unsuitable for large-scale application, and heavy metals and chlorine salts present in fly ash interfere with basic hydration reactions of cement, leading to an inadequate setting and/or deterioration of S/S [5–7].

Compared with the above treatment methods, hydrothermal solidification for processing of fly ash is regarded as promising technology, because it might have substantial advantages in terms of economic, technical, and environmental performance [8]. Under hydrothermal conditions, the ion product of water is thousands of times that at room temperature and pressure, so the reaction rate will be increased substantially, so hydrothermal processes that take millions of years during diagenesis of sedimentary rocks occur within a short period in the laboratory. For this reason, MSWI fly ash might be solidified hydrothermally into a very tough and durable product. Moreover, energy consumption during hydrothermal solidification (150 °C) is approximately 2.7 GJ/m$^3$ which is 1/6 of that required for traditional sintering of ceramic tiles. The hydrothermal processing technique has been used to treat metal-contaminated soil, convert concrete waste into construction materials, and to solidify coal fly ash and MSWI bottom ash [9–11]. To the best of our knowledge, however, little research on hydrothermal solidification of MSWI fly ash has been reported. The objectives of this work were to investigate how to recycle MSWI fly ash by hydrothermal solidification, how to improve the reactivity of MSWI fly ash by mixing with NaOH solution and by pre-washing treatment, and the effects of quartz addition, curing temperature, and time on strength development of solidified MSWI fly ash specimens. In order to expand the scope of recycling of fly ash, fly ash was also investigated as an additive for solidifying MSWI bottom ash. The study is expected to provide fundamental information for assessment of the feasibility of reusing MSWI fly ash on a large scale by use of the hydrothermal processing technique.

## Experimental

### Materials and preparation

The MSWI fly ash and bottom ash used were obtained from an incineration plant in Shanghai, China. The MSWI fly ash was used as raw material directly, whereas the

MSWI bottom ash was ground with a ball mill to pass 100 mesh. In order to remove as much chloride as possible, the MSWI fly ash was pretreated by water-washing at 400 rpm for 30 min in a glass beaker equipped with a magnetic stirrer for mixing. The distilled water to solid mass ratio (mL/g) used was five. Subsequently, this mixture was filtered by use of a frame filter press with a 0.45 mm membrane and the residue was dried at 80 °C for use. The chemical compositions and particle size distributions of the washed fly ash and bottom ash were determined by X-ray fluorescence (XRF) (model RIX3100, Rigaku) and laser particle-size analysis (LPSA) (model X100, Microtrac), respectively.

### Hydrothermal solidification

The washed fly ash mixed with quartz at different ratios was used as starting material. AR quartz was used as additive in this study. Distilled water or 2 M NaOH solution was added to the starting material as a reaction solution. The starting materials were firstly mixed with the reaction solution in a mortar by hand, and then the mixture was compacted by uniaxial pressing in a rectangular-shaped mold with compaction pressure of 30 MPa. The demolded green specimens were subsequently autoclaved under saturated steam pressure at 0–250 °C for up to 48 h. After autoclaving, all the solidified specimens were dried at 80 °C for 24 h before testing.

### Analysis

The dried rectangular-shaped specimens (35 mm length × 15 mm width × 8 mm height) were used to determine flexural strength, by use of a universal testing machine (Model XQ160-A). At least three specimens were tested for each hydrothermal processing condition. The strength results presented here are averages from three measurements obtained for three different specimens. The crushed specimens were then investigated by use of several analytical techniques: for crystalline phase analysis, X-ray diffraction (XRD) (model D/max2550VB3 +/PC); for microscopic morphology, scanning electron microscopy (SEM) (model Quanta 200 FEG); for microstructure, Fourier transform infrared spectroscopy (FTIR) (model EquinoxSS/Hyperion200); for heavy metals dissolved from the solidified specimens, inductively coupled plasma-mass spectrometry (ICP–MS). The leaching tests were conducted in accordance with the standard for pollution control on landfill sites for municipal solid waste in China (GB16889-2008), by the standard method for leaching toxicity of solid wastes, "Roll over leaching procedure" (GB5086.1-1997).

## Results and discussion

### Material characterization

The particle size distributions of raw fly ash and bottom ash are shown in Fig. 1; their average D(50) particle sizes (50% of the particle sizes are smaller than this

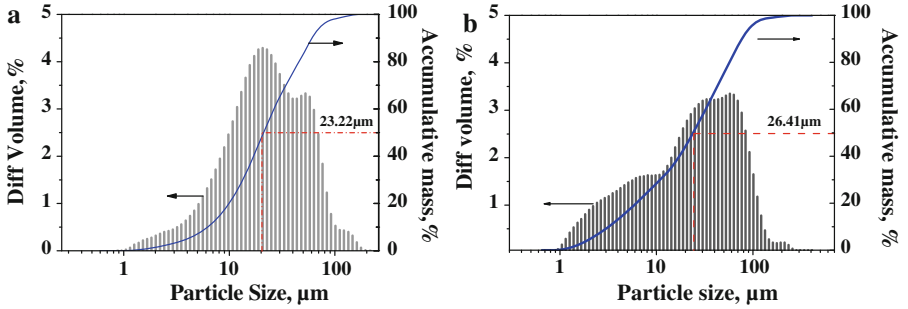


**Fig. 1** Particle size distributions of **a** raw fly ash and **b** bottom ash

value) are 23.22 and 26.41 μm, respectively. The chemical compositions of the raw fly ash, washed fly ash, and bottom ash are presented in Table 1. Note that for raw fly ash there are large amounts of Ca whereas amounts of Si are low; there are, moreover, large amounts of Cl. After washing, however, the Cl content of fly ash has dropped sharply from 20.5 to 3.09%, which indicates that the effect of washing on removal of Cl is distinct. The mineralogical compositions of the raw and washed fly ash measured by XRD are shown in Figs. 2 and 3. The phases of these correspond chiefly to calcium chloride hydroxide (CaClOH), sylvite (KCl), portlandite ($Ca(OH)_2$), halite(NaCl), and calcium sulfate ($CaSO_4$).

Cl clearly exists in the form of soluble salts, for example NaCl, KCl, and CaClOH. After washing, the peak intensities of these soluble salts decrease substantially. The phases of bottom ash are mainly quartz ($SiO_2$), calcite ($CaCO_3$), anhydrite ($CaSO_4$), and feldspar ($R(AlSi_3O_8)$) (R:Alkali metal) [12, 13].

## Effect of addition of quartz

Our previous work showed that tobermorite formation could improve the strength of hydrothermally solidified specimens [14, 15]. Tobermorite, a calcium silicate hydrate mineral of ideal composition $Ca_5Si_6H_2O_{18}{\cdot}4H_2O$, is very rare naturally but can be synthesized by hydrothermal processes [15]. According to Table 1, addition of quartz may promote tobermorite formation because of the low Si content of the raw fly ash. The effect of the amount of quartz on the flexural strength of specimens solidified at 200 °C for 12 h with 10% $H_2O$ was investigated first.

Figure 4 shows that flexural strength, as expected, initially increases on addition of quartz, and at a $CaO/SiO_2$ molar ratio (Ca/Si) of 0.7 reaches its highest value, near 14 MPa, and then starts to decline. It is well known that the normal Ca/Si for tobermorite is 0.83. So we speculate that strength development of the solidified specimens is because of tobermorite formation. Ca/Si = 0.7 was selected for further study.

The phase evolution for the above specimens was investigated by XRD analysis (Fig. 5), and the mineralogical composition for the washed fly ash (Ca/Si = 4.5) confirmed the main phases corresponded to portlandite ($Ca(OH)_2$), anhydrite ($CaSO_4$), and tobermorite. Compared with the XRD pattern of the washed fly ash

**Table 1** Composition of raw fly ash, washed fly ash, and bottom ash

| | Raw fly ash (%) | Washed fly ash (%) | Bottom ash (%) |
|---|---|---|---|
| CaO | 46.8 | 50.2 | 27.9 |
| $SiO_2$ | 8.79 | 11.2 | 35.5 |
| Cl | 20.5 | 3.09 | 1.24 |
| $Na_2O$ | 4.38 | 0.76 | 2.69 |
| MgO | 1.57 | 2.25 | 2.61 |
| $Al_2O_3$ | 2.59 | 3.18 | 6.73 |
| $P_2O_5$ | 1.2 | 1.61 | 4.74 |
| $SO_3$ | 5.96 | 7.24 | 6.32 |
| $K_2O$ | 4.93 | 0.9 | 1.72 |
| $TiO_2$ | 0.46 | 0.14 | 0.78 |
| $MnO_2$ | 0.04 | 0.06 | 0.08 |
| $Fe_2O_3$ | 0.92 | 1.21 | 3.73 |
| CuO | 0.08 | 0.09 | 0.09 |
| ZnO | 0.59 | 0.79 | 0.37 |
| SrO | 0.04 | 0.04 | 0.07 |
| PbO | 0.25 | 0.12 | 0.12 |
| $Cr_2O_3$ | – | – | 0.02 |
| $SnO_2$ | – | – | 0.13 |

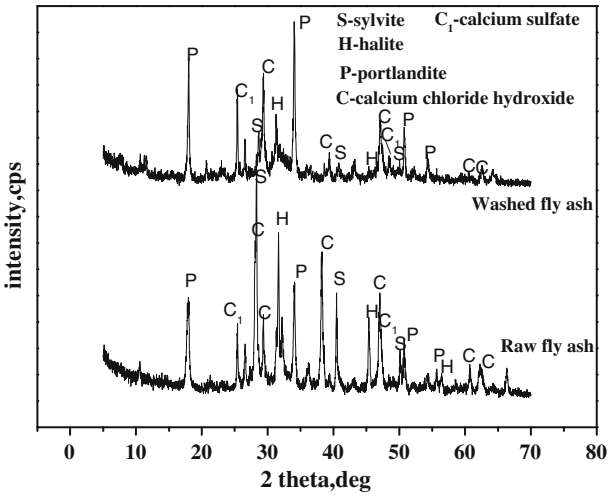


**Fig. 2** XRD patterns of raw fly ash and washed fly ash

shown in Fig. 2, even without any additions (Ca/Si = 4.5), a trace of a peak corresponding to 1.1 nm tobermorite forms after curing. With increasing quartz content (Ca/Si), portlandite peaks disappear and simultaneously the peak intensity of tobermorite becomes stronger and stronger. Comparison of the phase evolution with strength development (Fig. 4) shows that tobermorite formation does cause

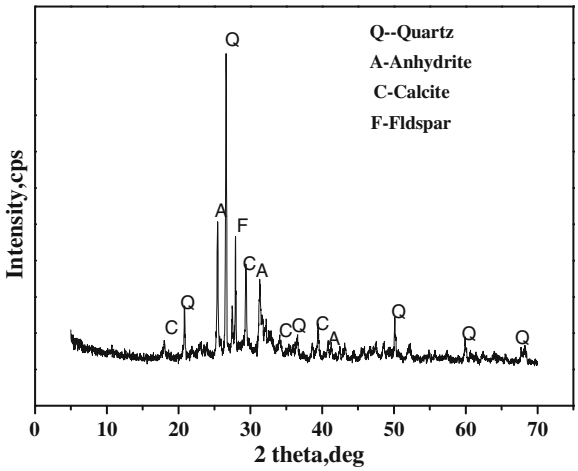


**Fig. 3** XRD patterns of bottom ash

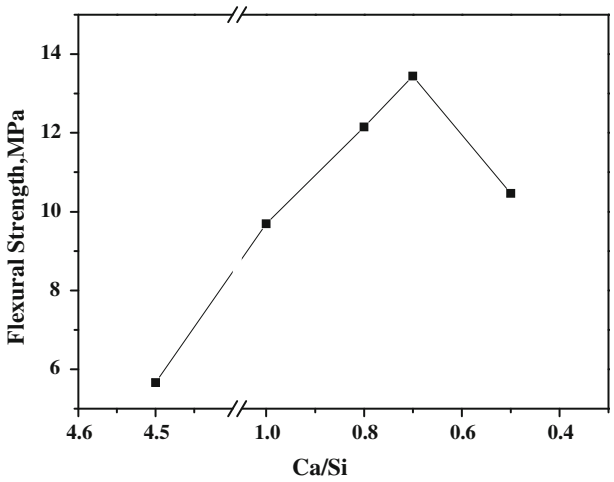


**Fig. 4** Effect of amount of quartz added. Hydrothermal processing conditions: water content 10% *m*/*m*; curing temperature 200 °C; curing time 12 h

strength development. The added quartz has reacted with portlandite to form tobermorite clearly, however, over-addition of quartz seems to be unfavorable for further hydrothermal reaction, and in turn, leads to a decrease in strength, which is in agreement with the work reported by Jing [16, 17].

## Effect of NaOH solution

It is generally accepted that hydrothermal reaction between silica and lime is mainly controlled by the solubility of silica, and the solubility of silica is enhanced at higher

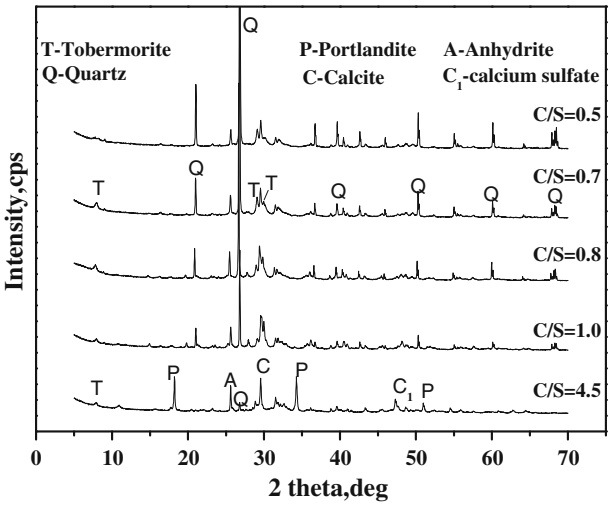


**Fig. 5** XRD patterns for solidified bodies with different quartz content. Hydrothermal processing conditions: water content 10% *m*/*m*; curing temperature 200 °C; curing time: 12 h

pH [10]. Therefore, the effect of the amount of NaOH solution (2 M) on the strength of the solidified specimens was also studied. Figure 6 shows that the strength of specimens solidified at 200 °C for 12 h increases quickly until the amount of NaOH solution reaches 15% *m*/*m*, and then decreases. Although the strength for $H_2O$ added is higher than that for NaOH added, the maximum strength (15 MPa) for NaOH solution added is higher than that for addition of $H_2O$. This suggests that not only pH but also amount of reaction solvent has an important effect on strength development.

In order to further investigate the mechanism of strength development, XRD phase evolution for different NaOH solution contents was also investigated. As Fig. 7a shows, calcite, anhydrite, quartz, and tobermorite exist in all specimens; the peak intensity, however, particularly for the tobermorite peak, is different. At an NaOH solution content of 15%, the peak intensity of tobermorite is highest, which may lead to the highest strength shown in Fig. 6. A high pH makes more silicon available for reaction with calcium to form tobermorite; however, tobermorite formation also seems to be related to the NaOH content of the solution. From Fig. 7b, The peak intensity of tobermorite for 15% *m*/*m* NaOH solution is also higher than that for 15% *m*/*m* water, which shows that 15% *m*/*m* NaOH solution is more favorable for the tobermorite formation and in turn results in a higher strength (Fig. 6).

## Effect of curing time

In order to elucidate the hardening mechanism during the hydrothermal process, the effect of curing time on the strength of specimens solidified at 200 °C was investigated. Figure 8 shows that the flexural strength increases with increasing

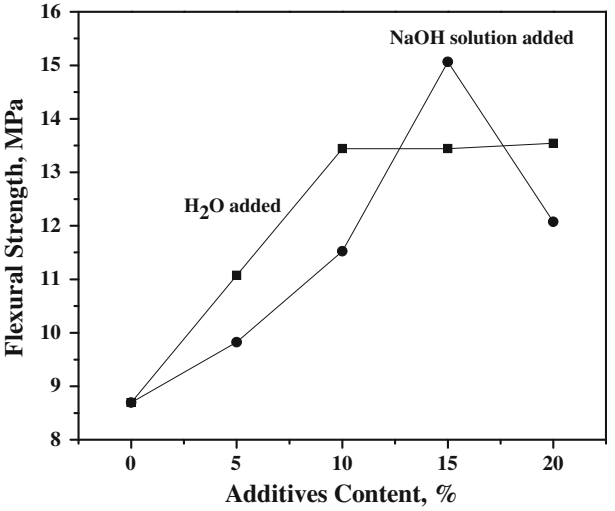


**Fig. 6** Effect of water content and NaOH solution on the flexural strength of solidified bodies. Hydrothermal processing conditions: Ca/Si = 0.7; curing temperature 200 °C; curing time: 12 h

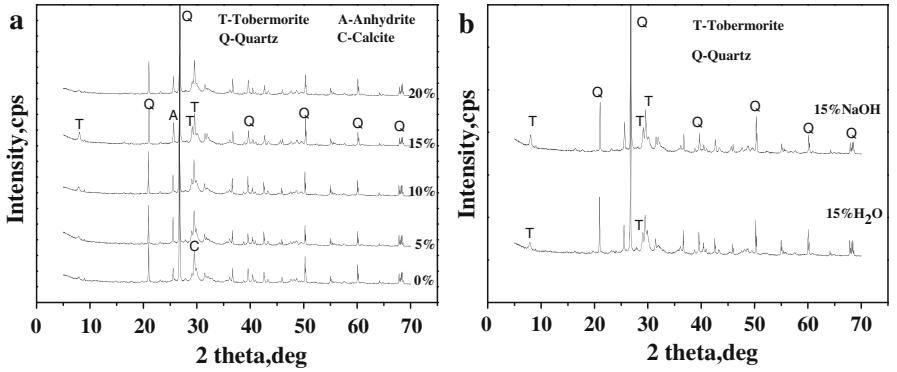


**Fig. 7** XRD patterns of solidified bodies with **a** different amounts of NaOH solution (2 M) and **b** comparison of 15% *m/m* $H_2O$ and 15% *m/m* NaOH solution. Hydrothermal processing conditions: Ca/Si = 0.7; curing temperature 200 °C; curing time 12 h

curing time up to 12 h, then declines gradually afterwards. XRD analysis (Fig. 9) reveals the phase evolution during this process. At 0 h (without hydrothermal processing), the phases are mainly portlandite, calcite, and anhydrite. From 3 h, new phases corresponding to 1.1 nm tobermorite and CSH gel tend to be distinct, while the portlandite peak is no longer observed, which suggests a transformation from $Ca(OH)_2$ to tobermorite. At 12 h, the peak intensity of tobermorite becomes highest, and afterwards, the peak intensity of tobermorite seems to decrease, which shows that an excessive curing time has a negative effect on tobermorite formation and thus reduces strength development (Fig. 8).

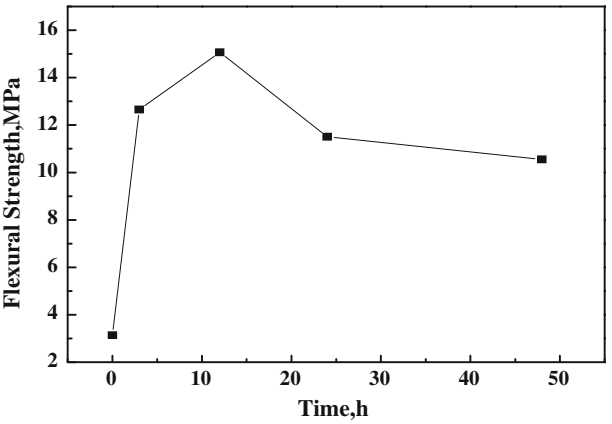


**Fig. 8** Effect of curing time on flexural strength of solidified bodies. Hydrothermal processing conditions: Ca/Si = 0.7; NaOH solution content 15% *m*/*m*; curing temperature 200 °C

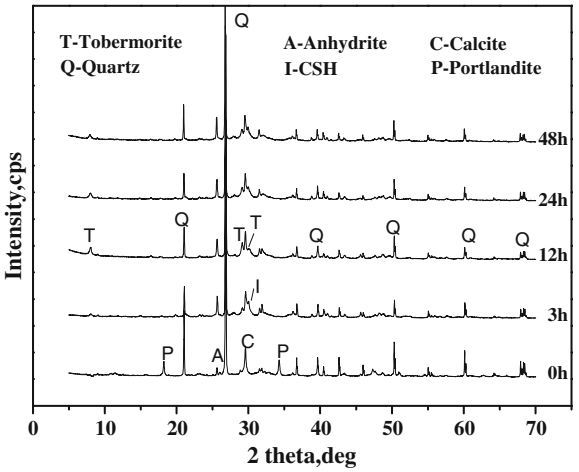


**Fig. 9** XRD patterns of solidified bodies cured for different times. Hydrothermal processing conditions: Ca/Si = 0.7; NaOH solution content 15% *m*/*m*; curing temperature 200 °C

The micro-surroundings of the structures of the reaction products were also characterized by Fourier transform infrared (FTIR) spectroscopy. As seen in Fig. 10, there is a band at 3,644 $cm^{-1}$ at 0 h, which is caused by vibration of O–H bonds. From 3 h, the band tends to disappear. According to XRD analysis shown in Fig. 9, the O–H band should mainly belong to $Ca(OH)_2$. At the same time, the band corresponding to Si–O stretching vibration in quartz, appears at about 779 $cm^{-1}$, and with curing time the band tends to become weak, suggesting a reaction progress between $Ca(OH)_2$ and $SiO_2$. The broad peak at 800–1,200 $cm^{-1}$ is caused by asymmetric stretching vibration of O–Si–O and Si–O–Si in the matrix. From 3 h,

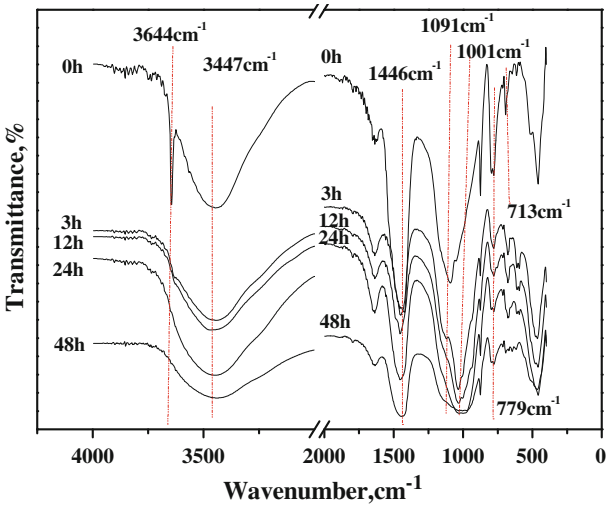


**Fig. 10** IR patterns of solidified bodies cured for different timed. Hydrothermal processing conditions: Ca/Si = 0.7; NaOH solution content 15% *m*/*m*; curing temperature 200 °C

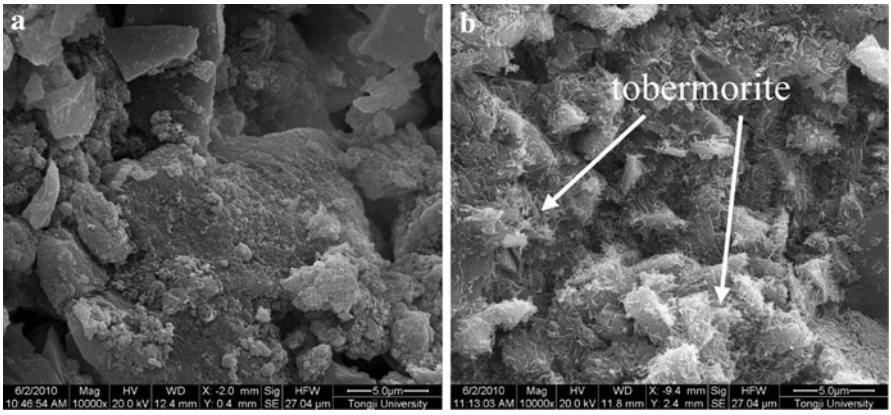


**Fig. 11** SEM photographs of solidified bodies cured at 200 °C for 0 h (**a**) and 12 h (**b**)

the broad peak of 1,091 $cm^{-1}$ shrinks and gradually shifts to a position of lower wave number, which may be because of the formation of CSH gel [1]. At 12 h, the peak moves to 1,001 $cm^{-1}$ and its intensity reaches its highest. This band corresponding to Si–O stretching may be caused by the tobermorite formed, which is in agreement with other research [18]. However, from 24 h, the peak tends to shift back to higher wavenumber again, which indicates that a longer curing time is unfavorable for tobermorite formation, and this leads to the strength reduction (Fig. 8). These findings match well with the results obtained from XRD analysis.

Figure 11 shows SEM photographs obtained from specimens solidified at 200 °C for (a) 0 h and (b) 12 h. From Fig. 11a, the internal accumulation structure within

the green specimens is disorganized and loose. However, after hydrothermal processing, newly formed crystals (tobermorite) fill the space between fly ash particles, which makes the matrix dense and thus enhances its strength.

### Effect of curing temperature

The curing temperature also affects strength development. Figure 12 shows that the strength does not increase below 100 °C, then increases until 200 °C and decreases for higher curing temperature.

Phase evolution with curing temperature was also analyzed by XRD. Figure 13 shows that there seems to be no difference in XRD phases between 0 and 100 °C. From 150 °C, the peak of portlandite disappears suggesting some reaction has occurred, and at 200 °C a new phase corresponding to 1.1 nm tobermorite forms. However, at 250 °C, the peak intensity of tobermorite decreases. The phase evolution for tobermorite seems to agree with the strength development (Fig. 12).

### Effect of washing

The chlorine content affects the strength of hydrothermally solidified specimens negatively. In order to investigate the washing effect, comparison of raw fly ash with washed fly ash as raw materials was conducted for different NaOH solution contents. From Fig. 14, strength development for washed fly ash is higher than that for raw fly ash, and the largest increase reaches approximately 4 MPa.

In raw fly ash there are large amounts of Cl ion. During hydrothermal processing, Ca ion tends to react with Cl ion to form $CaCl_2$ instead of Si ion to form tobermorite (or CSH gel) because of the low formation energy of $CaCl_2$. This leads to a low strength.

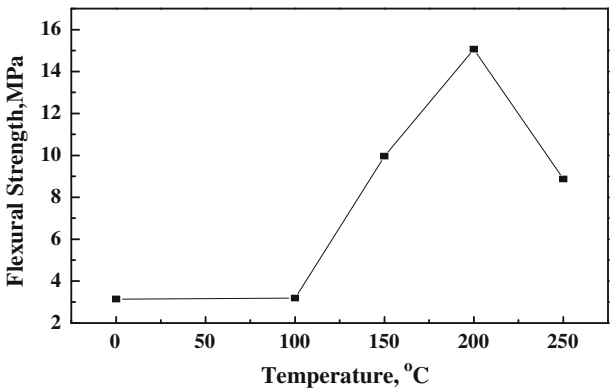


**Fig. 12** Effect of curing temperature on the strength of solidified bodies. Hydrothermal processing conditions: Ca/Si = 0.7; NaOH solution content 15% *m*/*m*; curing time 12 h

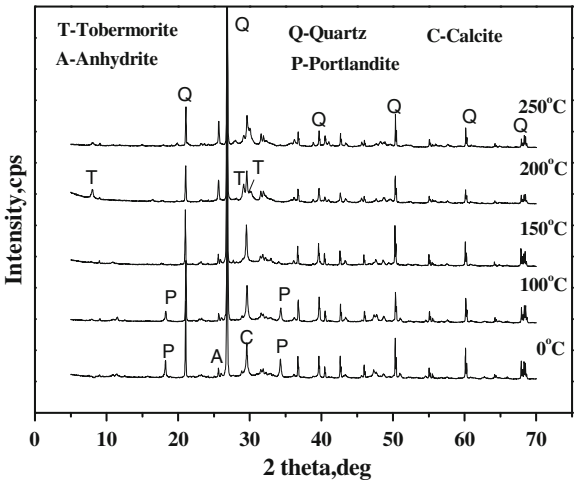


**Fig. 13** XRD patterns of the solidified bodies cured at different temperature. Hydrothermal processing conditions: Ca/Si = 0.7; NaOH solution content 15% *m*/*m*; curing time 12 h

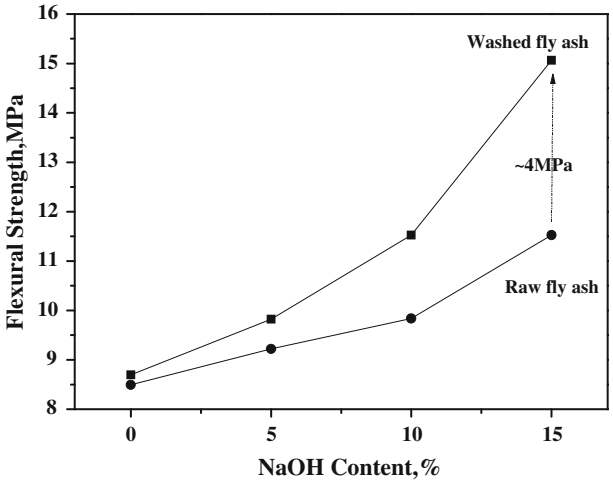


**Fig. 14** Comparison of raw fly ash and washed fly ash, with different NaOH solution content, on strength development. Hydrothermal processing conditions: Ca/Si = 0.7; curing time 12 h; temperature: 200 °C

## Effect of raw fly ash as an additive for solidifying bottom ash

In Table 1, because the $SiO_2$ content of bottom ash is higher than the CaO content, slaked lime could be added to bottom ash for hydrothermal reaction to form tobermorite. Note that the CaO content of raw fly ash is much higher than the $SiO_2$ content, and therefore the raw fly ash might have potential as an additive for bottom ash solidification, similar to addition of slaked lime. Figure 15 shows the effect of

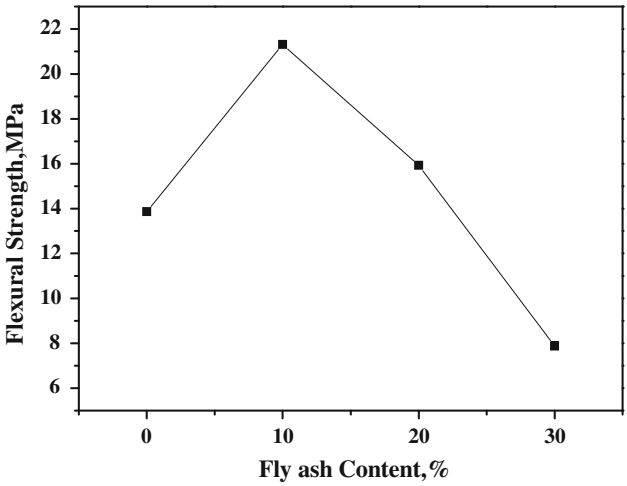


**Fig. 15** Effect of fly ash as an additive in solidifying bottom ash. Hydrothermal processing conditions: $H_2O$ content 15% *m/m*; curing time 12 h; temperature 200 °C

adding raw fly ash on strength development of bottom ash specimens. The strength, as expected, increases substantially at first and then decreases for a large content of raw fly ash. At 10% *m/m* fly ash, the flexural strength of solidified bodies reaches 21 MPa, which is much higher than that of ordinary concrete products. This suggests there is high potential to recycle 100% MSWI ash as 10% fly ash + 90% bottom ash.

Figure 16 indicates the evolution of XRD patterns for the strength development shown in Fig. 15. Evolution of the peak intensity of tobermorite matches well with strength development, and the more tobermorite formed, the higher the strength achieved. At 30% *m/m* fly ash additions, the peak of tobermorite is no longer observed, which also causes the low strength in Fig. 15

## Leaching test

Generally, the environment consequences of utilization of wastes are associates mainly with release of contaminants by percolating water. Therefore, a leaching test was carried out to determine the amount of heavy metals dissolved from the solidified bodies. Table 2 shows the leaching results of the washed fly ash and solidified specimens at 200 °C for 12 h with Ca/Si = 0.7 and 15% *m/m* NaOH solution (2 M). The heavy metal concentrations marked "a" and "b" were detected by ICP and ICP-MS, respectively.

Although the concentrations of heavy metals dissolved from the washed fly ash are high (e.g. Pb 50.745 ppm), after hydrothermal processing the amount of dissolved heavy metals becomes low, well below the regulatory level for the environmental quality standards of China (GB16889-2008), thus suggesting that hydrothermal solidification, at least under the conditions Ca/Si = 0.7, 15%

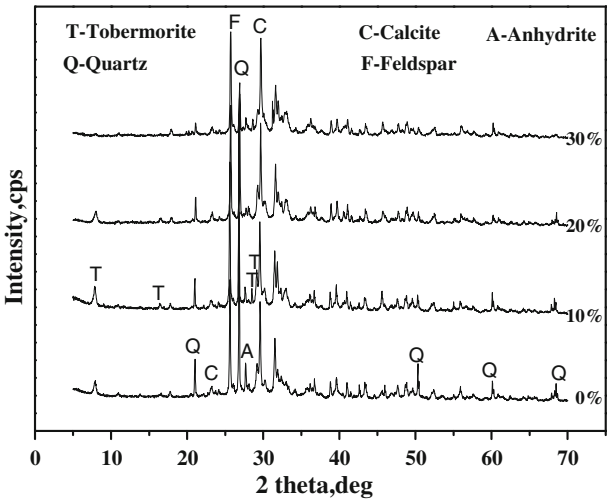


**Fig. 16** XRD patterns of the solidified bodies using bottom ash with fly ash as an additive. Hydrothermal processing conditions: $H_2O$ content 15% *m*/*m*; curing time 12 h; temperature 200 °C

**Table 2** Leaching test results of solidified bodies (ppm)

| Component | Washed fly ash | Specimen |
|---|---|---|
| Pb[a] | 50.745 | 0.19 |
| Cr($Cr^{3+}$ + $Cr^{6+}$)[b] | 0.224 | 0.123 |
| Ni[b] | 0.0006 | 0.0003 |
| Hg[b] | <0.05 | <0.05 |
| Se[b] | 0.111 | 0.032 |
| Ba[b] | 1.114 | 0.045 |
| Cd[b] | 0.027 | 0.009 |
| As[b] | 0.13 | 0.07 |

[a] The value was determined by ICP

[b] The values were determined by ICP-MS

*m*/*m* NaOH solution, curing temperature 200 °C, and time 12 h, has the capability of fixing heavy metals in the material of the solidified specimen.

The detailed mechanism for fixing the trace heavy metals in hydrothermal specimens is not fully understood. However, some possibilities may prevent dissolution of heavy metals. The tobermorite formed may exert a significant effect on fixing the heavy metals in the solidified specimens. Komarneni and Roy [19] reported the tobermorites were a new family of cation exchangers and Komarneni also pointed out that tobermorite was extremely efficient in the removal of all the heavy metals except $Cr^{6+}$, and was superior to zeolites [20, 21]. In this study, the leaching tests were conducted under laboratory conditions, and so the results may be difficult to reproduce on a large scale. Still, this study seems to provide a method for fixing heavy metals by solidification of fly ash that is worthy of further study.

## Conclusions

Hydrothermal solidification of MSWI fly ash has been carried out, and the experimental results of this study can be summarized as follows:

1) The most important strength-producing constituent in the solidified bodies was found to be tobermorite, and quartz addition promoted tobermorite formation.
2) Addition of NaOH solution (2 M) enhanced the strength of solidified specimens because a higher pH results in a greater solubility of silica, which promotes tobermorite formation.
3) Curing time and temperature favored reaction between Si and Ca, and this improved strength development. A curing time that was too long or a curing temperature that was too high, however, had a negative effect on tobermorite formation, which reduced strength development.
4) Fly ash could be used as an additive to solidify MSWI bottom ash, and with 10% *m*/*m* addition, the flexural strength of solidified specimens reached more than 21 MPa. This suggests that there is a high potential to recycle 100% MSWI ash as 10% fly ash + 90% bottom ash.
5) After hydrothermal processing the concentration of heavy metals dissolved from the solidified specimens was reduced effectively. As such, the hydrothermal processing may have high potential for recycling/reusing fly ash on a large scale.

**Acknowledgments** The work reported here was supported by the Shanghai Pujiang Program (China) (no. 08PJ14098), Shanghai Science and Technology Committee Program (China) (no. 09JC1413900), and the National Natural Science Foundation of China (no. 50872096, 51072138).

## References

1. G.-R. Qian, Y.-L. Cao, P.-C. Chui, J. Tay, J. Hazard. Mater. B **129**, 274 (2006)
2. Y.J. Park, J. Heo, J. Hazard. Mater. **91**, 83 (2002)
3. K.J. Hong, S. Tokunaga, T. Kajiuchi, J. Hazard. Mater. **75**, 57 (2000)
4. F.P. Glasser, J. Hazard. Mater. **52**, 151 (1997)
5. A.P. Bayuseno, W.W. Schmahl, T. Müllejans, J. Hazard. Mater. **167**, 250 (2009)
6. M. Ahmaruzzaman, Prog. Energy Combust. Sci. **36**, 327 (2009)
7. A. Nzihou, P. Sharrock, Waste Manage. **22**, 235 (2002)
8. C. Ferreira, A. Ribeiro, L. Ottosen, J. Hazard. Mater. **96**, 201 (2003)
9. T. Ida, N. Nakao, T. Tanaka, R&D Kobe Steel Eng. Rep. **53**, 111 (2003) (in Japanese)
10. Z.-Z. Jing, N. Matsuoka, F.-M. Jin, N. Yamasaki, Mater. Sci. **41**, 1579 (2006)
11. Z.-Z. Jing, N. Matsuoka, F.-M. Jin, T. Hashida, Waste Manage. **27**, 287 (2007)
12. Y.-S. Liu, L.-T. Zheng, X. Li, S. Xie, J. Hazard. Mater. **162**, 161 (2009)
13. J.-L. Xie, Y.-Y. Hu, D.-Z. Chen, B. Zhou, J. Front, Environ. Sci. Eng. **4**, 108 (2010)
14. Z.-Z. Jing, F.-M. Jin, T. Hashida, N. Yamasaki, E.H. Ishida, J. Mater. Sci. **43**, 2356 (2008)
15. Z.-Z. Jing, F.-M. Jin, N. Yamasaki, E.H. Ishida, J. Am. Chem. Soc. **46**, 2657 (2007)
16. Z.-Z. Jing, X.-Q. Ran, F.-M. Jin, E.H. Ishida, J. Waste Manage. **30**, 1521 (2010)
17. Z.-Z. Jing, F.-M. Jin, T. Hashida, N. Yamasaki, J. Mater. Sci. **42**, 8236 (2007)
18. N.Y. Mostafa, A.A. Shaltout, H. Omar, S.A. Abo-El-Enein, J. Alloy Compd. **467**, 332 (2009)
19. S. Komarneni, D.M. Roy, J. Sci. **221**, 647 (1983)
20. S. Komarneni, J. Waste Manage. **5**, 247 (1985)
21. F.-S. Zhang, H. Itoh, J. Hazard. Mater. **B136**, 663 (2006)